EUROPEAN ORGANIZATION FOR NUCLEAR RESEARCH

PS/AA/84-12
September 1984

SOME MONTE CARLO ANTIPROTON YIELD CALCULATIONS FOR AA

Steve Hancock

ABSTRACT

A series of Monte Carlo calculations has been performed to optimize simultaneously some of the parameters of various target-horn combinations for the production of antiprotons in AA. A summary is presented of those variables examined together with the optimum antiproton yield computed for each configuration treated.

1 BACKGROUND

The origins of the Monte Carlo program employed in the present investigation lie with Simon van der Meer. Originally conceived as just a subroutine, gross simplifications were made to enable MINUIT optimizations to be performed with reasonable convergence times. The profile of the "standard horn" currently installed in AA was itself developed using this early routine.

Ray Sherwood has been responsible for greatly increasing the sophistication of the program. Important contributions have included a more accurate parametrization of the angular production spectrum for antiprotons and, for example, the introduction of multiple Coulomb scattering. More recently, the program has developed new appendages to cope with a conducting target and to model the action of an upstream lithium lens.

The purpose of the present study has been not only to re-assess, using Ray's full-blown Monte Carlo, the possibility of improving the current AA performance, but also to evaluate the relative merits of a short focal length magnetic horn. The design of the new horn has been derived from analytic considerations by Jean-Claude Schnuriger, who proposes its use, in conjunction with a conducting target, ultimately to satisfy the antiproton production demands made by ACOL[1].

1.1 ESSENTIAL FEATURES OF THE MONTE CARLO PROGRAM

In its present form, the program ray traces particles stepwise through the magnetic fields of a given target-horn configuration. The increments are made in r (i.e. transversely) and numerical integration yields the corresponding steps in z (the beam direction). Axial symmetry is assumed in order to reduce the problem to simply tracking in r and z by removing the significance of the ϕ-dependence from the equations of motion. This does however preclude any estimation of alignment tolerances, since an off-axis target rod cannot be simulated.

The incoming protons are scattered in the various materials of a coaxially-structured target assembly, or they may interact to produce antiprotons which, in turn, are scattered or may be re-absorbed. For obvious economy of computing time, each proton interaction is assumed to produce an antiproton so that this production rate must be renormalized according to the number of Monte Carlo interactions in, and the production cross-section for, each of the materials comprising the target assembly. The final result is a yield figure giving the number of antiprotons that get into the required acceptance per proton in the incoming beam.

The target may also support a specified current. Total field penetration is then assumed. In such conducting target cases, it is

also possible to "switch on" an idealized upstream lithium lens. This prefocusing increases the convergence of the incoming beam envelope such that the defocusing effect of the target current is exactly matched and the beam necks at the centre of the target with the desired radius and emittance. In the absence of prefocusing the starting conditions for antiproton generation are taken as those for the passive case, so that the beam, which would indeed neck with the required dimensions were the target current zero, blows up when the target is pulsed.

1.2 THE PARAMETER LIST

The emergence of a more and more sophisticated Monte Carlo program has seen a concomitant increase in the size of the parameter list required for program flexibility. This dataset currently stands at over forty parameters, although several of these are fixed by the design of the AA machine itself while others are experimentally-determined data such as production cross-sections.

The optimization of the free variables using some standard minimization routine is precluded as it now requires several CDC CPU seconds to process a single geometry. Nor, indeed, is it realistic to attempt an exhaustive investigation of such a multi-dimensional space by hand. Instead, the simultaneous optimization of those parameters most readily amenable to practical alteration has been performed - albeit by laborious manual iteration.

The "suck-it-and-see" parameters selected were the length of the target, its position relative to the magnetic horn and the aspect ratios of the transverse phase space ellipses of the AA acceptance immediately downstream of the horn. The dependence upon target current of the optimum target postion was also examined for those cases in which a conducting target was modelled.

For the purpose of following particle trajectories through the surfaces of the magnetic horn, it proves convenient to define the downstream end of the horn neck as the origin in z. Thus the postion of the target, as specified by the displacement of the downstream target face from this origin, was a parameter which was always negative.

The transverse acceptance of the AA machine was fixed at 90π mm.mrad horizontally and 80π mm.mrad vertically. Hence the aspect ratio of each of the transverse acceptance ellipses was determined by specifying the radial dimension. Right ellipses were assumed.

2 COMPUTED RESULTS

The optimum antiproton yield computed for each of the four basic configurations treated is given in table 1. The corresponding values of

those parameters as a function of which the optima were obtained are also tabulated. The quoted yield figures are normalized to 10^{13} protons in the incoming beam.

The nature of the casting technique available for the manufacture of continuous copper target rods imposed an upper limit of 115 mm on the length that could be considered for a conducting target. The true optimum was actually found to exceed this by some 25 mm in both the standard and the Schnuriger horn conducting target cases, but the dependence on target length was, anyway, generally fairly shallow.

A working limit was also imposed on the target current. The conducting target results of table 1 are for the maximum 140 kA current, while figures 1 and 2 display, for the standard and Schnuriger horn respectively, the dependence of yield on target position at reduced and, indeed, zero target current. For each horn, all the conducting target plots are for the same target length and the same acceptance matching as listed in table 1.

The prefocusing option was selected for all cases in which the target was pulsed.

Subjective curves are drawn in figures 1 and 2 as it would be extremely difficult to assess the combined significance of all the individual parameter tolerances. However, Poisson error bars due to the Monte Carlo statistics alone would extend roughly ±2%.

The results presented here pertain solely to copper targets.

3 DISCUSSION

It is evident from figures 1 and 2 that, while the Schnuriger horn has a shorter focal length than the standard one and so can capture particles emerging at larger angles from the target, it necessarily has less depth of focus in that it is more sensitive to target position. Now the focal length of a magnetic horn is non-trivially related both to the profile of the horn and to the horn current and, consequently, these were never considered to be free variables. The horn current was fixed at the design value of 250 kA for the Schnuriger horn, while it remained set at 160 kA for the standard horn in deference to the experience gained from the use of the latter in AA.

Table 1 indicates that the advantage of using the short focal length Schnuriger horn is lost once the target is pulsed. In an effort to understand this, an idealized Schnuriger horn was modelled with an extended profile according to the same theoretical function as the original such that the neck through its current-carrying surface was a mere pin-hole. This revealed that the class of particles which emanate from the conducting target at too small an angle to see the field in the

horn but at too large an angle to fall inside the acceptance constitutes almost 15% over and above the yield actually realized by the Schnuriger horn. Such particles are not as prevalent in the passive case, since there is no target field to start focusing the antiprotons towards the axis as soon as they are born.

The standard horn has a very short neck, but it too fails to capture particles in one particular region (off-axis at positive r') of phase space. This has been interpreted as indicative of a strong upstream-downstream asymmetry in the depth of focus of the standard horn.

Setting the radiation length of aluminium to infinity in the parameter list established that the loss in yield due to Coulomb scattering in the thin walls of the horn was a <3% effect in the Schnuriger case, rising to almost 10% in the standard one.

4 REFERENCE

1. J.C. Schnuriger, Proposal for a Reliable Solution of the Improved Production of Antiprotons for ACOL, CERN PS/AA/AC-21 (1984).

	Target Length /mm	Relative Target Position /cm	Transverse Acceptance Radii (H,V) /mm	Computed Yield / $\bar{p}$ per 10^{13} p
Standard Horn + Passive Target	120	-42	20,20	9.64×10^{6}
" + Pulsed (140 kA) Target	115*	-47	16,16	1.68×10^{7}
Schnuriger Horn + Passive Target	100	-25	17,17	1.18×10^{7}
" + Pulsed (140 kA) Target	115*	-30	14,14	1.75×10^{7}

*See section 2

Table 1

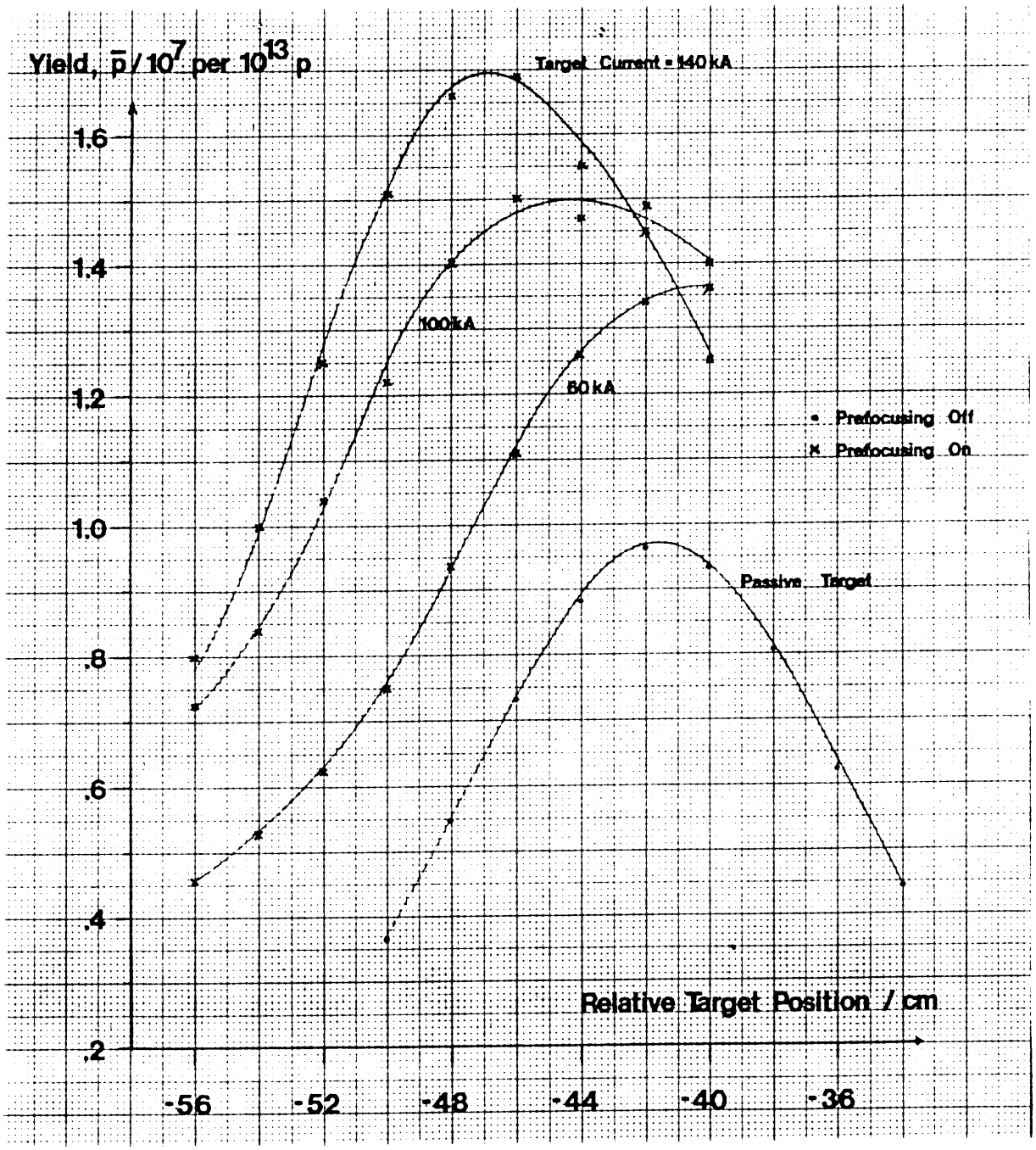

Figure 1. "Standard" Horn

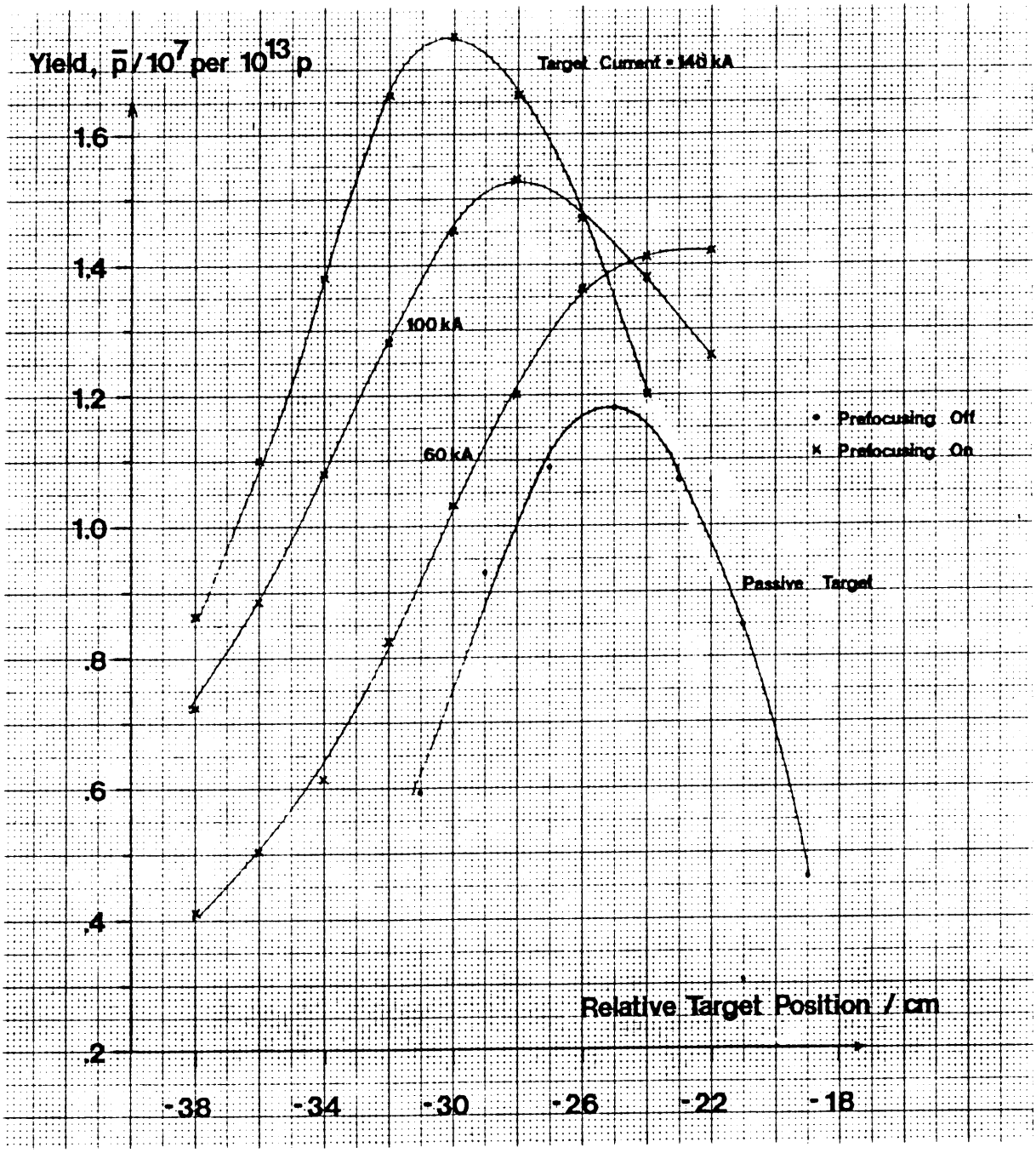

Figure 2. Schnuriger Horn